



**HAL**  
open science

# Spark Desensitization of Nanothermites via the Addition of Highly Electro-Conductive Carbon Particles

Pierre Gibot

► **To cite this version:**

Pierre Gibot. Spark Desensitization of Nanothermites via the Addition of Highly Electro-Conductive Carbon Particles. *Journal of Carbon Research*, 2022, 8 (3), pp.35. 10.3390/c8030035 . hal-03797040

**HAL Id: hal-03797040**

**<https://hal.science/hal-03797040v1>**

Submitted on 4 Oct 2022

**HAL** is a multi-disciplinary open access archive for the deposit and dissemination of scientific research documents, whether they are published or not. The documents may come from teaching and research institutions in France or abroad, or from public or private research centers.

L'archive ouverte pluridisciplinaire **HAL**, est destinée au dépôt et à la diffusion de documents scientifiques de niveau recherche, publiés ou non, émanant des établissements d'enseignement et de recherche français ou étrangers, des laboratoires publics ou privés.

# Spark Desensitization of Nanothermites via the Addition of Highly Electro-Conductive Carbon Particles

Pierre Gibot

NS3E Laboratory, UMR 3208 ISL/CNRS/UNISTRA, French-German Research Institute of Saint-Louis (ISL),  
5 rue du General Cassagnou, BP70034, 68301 Saint-Louis, France; pierre.gibot@cnrs.fr

**Abstract:** In the past decade, the formulation of spark-desensitized nanothermites has considerably advanced, making them safe to handle. When ignited, these materials reveal impressive properties such as high temperatures ( $>1000\text{ }^{\circ}\text{C}$ ), intense heat releases ( $>\text{kJ}/\text{cm}^3$ ), and sometimes gas generation. Unfortunately, these energetic systems are systematically characterized by an extreme sensitivity to electrostatic discharges, which can cause accidental ignitions during preparation, handling, and transport. The present study examines the electrostatic discharge sensitivity response of an Al/WO<sub>3</sub> energetic formulation doped with highly conductive carbon nanoparticles (Ketjenblack EC600JD). The results showed an increased threshold from  $<0.14\text{ mJ}$  to almost  $40\text{ mJ}$  with  $18.80\text{ vol. \%}$  of KB EC600JD in the energetic mixture. The energetic material was also desensitized to friction stress with a threshold greater than  $360\text{ N}$ , in contrast to a value of  $<4.9\text{ N}$  for an un-doped Al/WO<sub>3</sub> energetic composite material. The reactive performance of the system (w/o Ketjenblack additive) was verified in open medium by means of an optical igniter. The heat release was determined by a calorimetric bomb and a decrease of  $50\%$  was recorded for the carbon-doped energetic system compared to the pristine Al/WO<sub>3</sub> composition.

**Keywords:** Spark sensitivity; high-conductive carbon; nanothermites; desensitization

---

## 1. Introduction

Nanothermites are energetic composite materials that consist of physical mixtures of solid fuel and oxidizer nanoparticles. Upon ignition, a highly exothermic chemical reaction occurs w/o gaseous release. Aluminum is regularly used as a fuel. As an oxidizer component, a metal oxide can be used. For example, the aluminum (Al) and tungsten (VI) oxide (WO<sub>3</sub>) reacting pair generates a flame temperature and heat release as high as  $3253\text{ K}$  and  $2.9\text{ kJ/g}$  ( $15.9\text{ kJ}/\text{cm}^3$ ), respectively [1]. In addition to these reactive parameters, nanothermites, regardless of the fuel/metal oxide pair, present an extreme sensitivity to sparks (energy lower than  $1\text{ mJ}$ ) that can lead to accidental ignition by electrostatic discharge (ESD) and cause injury and damage. Therefore, the handling of these energetic composite materials requires specific care because the human body is a source of electrostatic energy [2,3]. Authors have determined the quantity of static electricity that can be generated by a human body to be mainly around  $8\text{--}20\text{ mJ}$ . Grounding is mandatory for operators in such an environment.

During the last decade, authors have worked on controlling the spark sensitivity of nanothermites by adding conductive (nano)charges. The goal is to increase the electrical conductivity of the energetic composite material. Thus, by creating a conductive device able to quickly dissipate electrostatic charges (bypassing the reactive components), the formation of hot spots (areas with a high energy density) between fuel and oxidizer nanoparticles is avoided and the ignition triggering is delayed. Higher stimuli energies are required to trigger nanoparticles. The additive should be inert to the thermite reaction and its concentration in the energetic material should be as low as possible, so that the overall pyrotechnic performance is not significantly changed. Among the conductive additives investigated—carbon, conductive polymers, and metals [4–14]—carbon structures such as nanotubes, graphene, graphite, and carbon black are efficient alternatives. For example, the Al/CuO energetic nanosystem could be desensitized to spark with an addition of  $13$

---

vol. % carbon nanotubes [4]. At this concentration, the electrical conductivity increased from  $9 \times 10^{-6}$  S/cm to 0.07 S/cm and more than 100 mJ is required to ignite the composite with a spark. The addition of graphite oxide (rGO) platelets has been studied in Al/Fe<sub>2</sub>O<sub>3</sub> nanothermites [5]. An ESD threshold of 24.5 mJ was measured with 9.6 wt. % of rGO, compared to a sensitivity value inferior to 2 mJ without graphite, but no reactive behaviour was examined by the authors. Pyrograph-III nanofibers were chosen as fillers in an Al/MnO<sub>2</sub> nanothermite [8]. By using carbon nanofibers (~ 40 wt. %) either as a matrix to precipitate the oxidizer MnO<sub>2</sub> or as a third independent component, the ESD sensitivity value was increased to values of 35 and 1800 mJ, respectively, compared to 1 mJ for the binary Al/MnO<sub>2</sub> energetic formulation. However, the reactive behaviour of the carbon-rich nanothermites was significantly decreased. The burning rate decreased from 730 mm/s to 3.5 and 5.1 m/sec, respectively, because of an overly high carbon concentration. A last example: nanodiamonds (NDs) have been added in an energetic Al/Bi<sub>2</sub>O<sub>3</sub> mixture [9]. The ESD sensitivity threshold was increased from <0.14 mJ to >20 mJ with the NDs' concentration below 3 wt. %, but the burning rate was also greatly decreased (500 m/s. vs. <100 m/s.) due to the combustion by-products (Al<sub>4</sub>C<sub>3</sub>) acting as a thermal barrier.

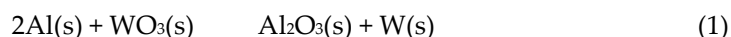
In the present work, highly conductive carbon nanoparticles (Ketjenblack carbon) were used as an additive in an Al/WO<sub>3</sub> nanothermite. The additive has a high electrical conductivity; therefore, it is expected to impact the ESD sensitivity of energetic composite materials. Ketjenblack material is used in a wide range of applications, including batteries (lithium- and sodium-ion), supercondensators, fuel cells, protective packaging for conductive paints, high-voltage cables, electronics, and safety clothes. It can also be implemented in many polymers to make them electrically conductive. In summary, the use of Ketjenblack nanoparticles is widely applicable. Moreover, Ketjenblack is easily available at a low cost and at a high degree of purity. The materials and the C-doped Al/WO<sub>3</sub> energetic formulations were characterized by transmission electron microscopy, nitrogen sorption, electrical conductivity measurements, and specific pyrotechnical tests (sensitivities to different stimuli, ignition, and combustion).

## 2. Materials and Methods

Tungsten (VI) oxide (WO<sub>3</sub>, 99.9%), aluminum (Al-50P, Al = 57.9%), and highly electro-conductive carbon black (C, Ketjenblack EC-600JD) nanopowders were supplied by the Sigma Aldrich, Nanotechnologies Inc. and AkzoNobel companies, respectively. Acetonitrile (CH<sub>3</sub>CN, 99%) was purchased from Roth. All chemical reagents were used as provided and without any further purification.

### 2.1. Formulation of the Carbon-Enriched Al/WO<sub>3</sub> Energetic Composites Materials

The Al/WO<sub>3</sub> energetic formulation, whose balanced chemical reaction is given in (1), was prepared by mixing the aluminum and tungsten (VI) oxide nanopowders in amounts defining an excess of fuel as leading to optimal performance.



The excess was defined by an equivalence ratio ( $\Phi$ ), detailed in Equation (2), equal to 1.4.

$$\Phi = \frac{\left(\frac{\text{F}}{\text{O}}\right)_{\text{exp.}}}{\left(\frac{\text{F}}{\text{O}}\right)_{\text{st.}}} \quad (2)$$

F and O represent the mass ratio of pure fuel (Al) to oxidizer (WO<sub>3</sub>), respectively, and the subscripts exp. and st. represent the experimental and stoichiometric ratios, respectively.

The amount of pure aluminum was calculated by subtracting the alumina amount (Al<sub>2</sub>O<sub>3</sub>) surrounding the particles (42.1 wt. %). Then, different amounts of conductive

---

carbon were added to prepare Al/WO<sub>3</sub>/C mixtures with 1, 2, 3, 5, 10, and 20 wt. % of carbon. From the weight % and density of each component, i.e., 7.16 g/cm<sup>3</sup>, 2.83 g/cm<sup>3</sup>, and 2.2 g/cm<sup>3</sup> for WO<sub>3</sub>, Al (surrounded by Al<sub>2</sub>O<sub>3</sub>), and C, respectively, and the theoretical maximum density (TMD) of the C-doped Al/WO<sub>3</sub> nanothermite considered, the vol. % of high-conductive carbon filler was calculated as equal to 2.1, 4.1, 6, 9.9, 18.8, and 34.2%. As a reminder, the TMD for a multi-material was calculated from Equation (3):

$$\text{TMD} = 1 / \sum_{i=1}^n \frac{X_i}{\rho_i} \quad (3)$$

where  $X$  and  $\rho$  represent the mass fraction and density, respectively, of the chemical  $i$ . The ingredients were mixed in 40 mL of acetonitrile and sonicated for 10 min. Acetonitrile was discarded using a rotary evaporator (200 mbar, 353 K). The resulting Al/WO<sub>3</sub>/C energetic composites were recovered and then placed in an oven at 353 K for 4 h before being stored in conductive boxes. For each nanothermites mixture, 500 mg was formulated.

## 2.2. Characterization Techniques

The structures of the materials and energetic composites were recorded by an X-ray diffraction analysis by means of a D8Advance diffractometer ( $\lambda_{\text{Cu}} = 1.54056 \text{ \AA}$ , working conditions 40 kV-40 mA) equipped with a Lynxeye detector (XRD, Bruker, Billerica, MA, USA). The XRD patterns were collected between  $2\Theta = 20\text{--}80^\circ$  coupled with a  $2\Theta$  step size of  $0.02^\circ$ . An InVia confocal Raman microscope (Renishaw, Wotton-under-Edge, UK) equipped with an argon ion laser ( $\lambda = 514 \text{ nm}$ ) was used. A calibration with a Si crystal was performed prior to analysis and the spectrum was collected in the range between  $900\text{--}2500 \text{ cm}^{-1}$ . The exposure time was about 50 s at a laser power of 1.25 mW. The Raman spectrum was fitted by means of the OriginPro Vers. 9 software (OriginLab Corp., Northampton, MA, USA) taking into account PseudoVoigt functions. A JEM 2100F transmission electron microscope (JEOL, Tokyo, Japan) at an acceleration voltage of 200 kV was used to observe the microstructures of the different materials. Specific surface area (SSA) of the materials were determined by nitrogen physisorption measurements at 77 K performed on an ASAP2020 apparatus (Micromeritics, Norcross, CA, USA). Analyses were performed on degassed samples (473 K, 6 h, vacuum  $< 10 \text{ \mu mHg}$ ) and the SSAs were determined considering the Brunauer–Emmet–Teller (BET) model applied in the 0.05–0.20 relative pressure domain. A two-probe method was used to measure the electrical conductivity of the materials. A Model 2010 low-noise multimeter (Keithley, Cleveland, OH, USA) was used and a description of the procedure that was followed is given in [11]. The mass of powder used for the test was similar for each sample, and the packing density was measured.

From a pyrotechnical point of view, the sensitivity properties and the reactive behaviour of Al/WO<sub>3</sub>/C nanothermites were determined. For the sensitivities, impact, friction, and electrostatic discharge stimuli were thus implemented. For this purpose, a BFH-12 drop hammer device, a FSKM-10 friction device, and a 2008 ESD tester, all from OZM Research, were used. A description of each tool and the measurement principles has been given in other papers [9,10,12]. Regarding the combustion events (ignition and burning) of Al/WO<sub>3</sub> nanothermites w/o high-conductivity carbon nanoparticles, the tests were performed (under a fume hood) using an optical flash device described in [10]. Typically,  $10 \pm 1 \text{ mg}$  of energetic nanocomposite was placed on a glass substrate ( $50 \text{ mm}^2$  surface area) held at a distance of 1 mm above the optical igniter (energy of  $0.11 \text{ J/cm}^2$ ). The progress of the combustion reaction was tracked by a high-speed FASTCAM camera system (Phantom, 105 frames/s, exposure time of 5  $\mu\text{sec}$ .) aligned perpendicular to the direction of frontal flame propagation. A C2000 IKA calorimeter with a C62 calorimetry bomb was used to determine the heat of the reaction of the energetic nanocomposites.

## 3. Results and Discussion

### 3.1. Characterizations of Individual Materials Constituting Al/WO<sub>3</sub>/C Energetic Formulations

The structure of the different materials used to formulate desensitized Al/WO<sub>3</sub>/C energetic composites was characterized by X-ray diffraction analysis. Figure 1 shows the X-ray diffraction patterns of aluminum (Al), tungsten (VI) oxide (WO<sub>3</sub>), and the highly-conductive carbon additive (EC-600JD) materials. Figure 1A shows the diffractogram of Al powder whose diffraction peaks were indexed in a cubic structure with the space group Fm-3m (JCPDS card No. 065-2869) as reported in the literature. The diffraction peaks of the WO<sub>3</sub> material (Figure 1B) were indexed into a monoclinic lattice with the P21/n space group corresponding to JCPDS card No. 43-1035. Finally, Figure 1C displays the structure of the carbon sample. Carbon exhibits a poor crystalline character because of the unresolved diffraction peak that was observed. Some Miller planes of the various crystalline materials have been plotted on each X-ray diffractogram. All samples were found to be pure.

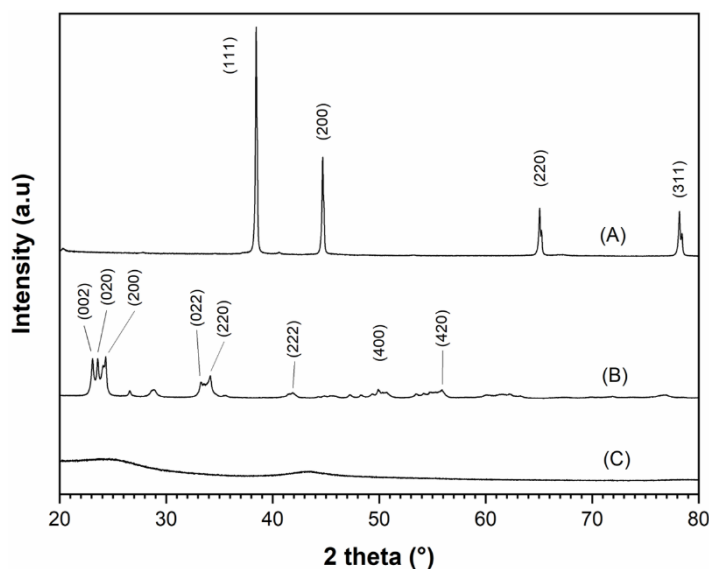


**Figure 1.** X-ray diffraction patterns of individual nanomaterials involved in Al/WO<sub>3</sub>/C energetic composites: (A) Al, (B) WO<sub>3</sub>, and (C) carbon (Ketjenblack EC-600JD).

To gain insight into the structure of the carbon additive (EC-600JD), a Raman spectroscopy analysis was performed. Figure 2 displays the representative spectrum. The spectrum shows two main contributions around 1340 cm<sup>-1</sup> and 1592 cm<sup>-1</sup> conventionally called D (Disorder) and G (Graphitic) bands, respectively [15]. The D band (A<sub>1g</sub> symmetry) corresponds to a carbon atom's vibration, or the atoms observed at the end of the graphite sheets. The G band (E<sub>2g</sub> symmetry) characterizes the sp<sup>2</sup>-carbon species in an in-plane stretching vibration. However, the deconvolution of the spectrum, performed using a PseudoVoigt function, shows four components; indeed, the G and D bands and two others attributed to sp<sup>3</sup>-carbons (~1188 cm<sup>-1</sup>) and amorphous carbon (1527 cm<sup>-1</sup>). The latter two are low intensity, in contrast to the G and D bands. The graphitization degree of highly conductive carbon, expressed from the intensities ratio of the fitted G and D bands (I<sub>D</sub>/I<sub>G</sub>), was found equal to 1.3. This value characterizes a disordered carbon material that agrees with the previous XRD analysis.

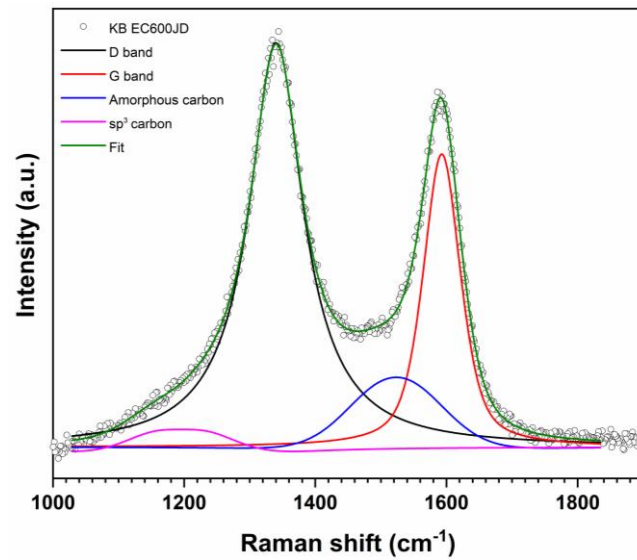


**Figure 2.** Raman spectrum of the carbon additive (Ketjenblack EC-600JD).

A transmission electron microscope (TEM) was used to image the microstructures (morphologies and particle sizes) of the different components (Figure 3). For the aluminum powder, Figure 3A,D show spherical particles with a size of about 50–100 nm. A core/shell structure characterizes the aluminum nanoparticles; indeed, as previously demonstrated in the literature [16], an alumina ( $\text{Al}_2\text{O}_3$ ) layer of a few nanometers (<4 nm) surrounds an aluminum core. This factual element is visible in the inset of Figure 3D. The tungsten (VI) oxide material consists of agglomerated particles that are systematically smaller than 50 nm (Figure 3B). The morphology is not precisely defined (Figure 3E). Then, for the Ketjenblack material, the unit particles have a quasi-spherical morphology (Figure 3C). From a magnified picture (Figure 3F), we could measure the size of the nanoparticles (smaller than 50 nm) and found that the nanoparticles have a strong interaction with each other. The microstructure reveals a disordered state supporting the XRD and Raman characterizations that were performed on this sample.

From nitrogen sorption measurements at 77K, the specific surface areas of each component were determined. Values of 45, 25, and 1302  $\text{m}^2/\text{g}$  were thus determined for the Al,  $\text{WO}_3$ , and carbon Ketjenblack EC-600JD samples, respectively.

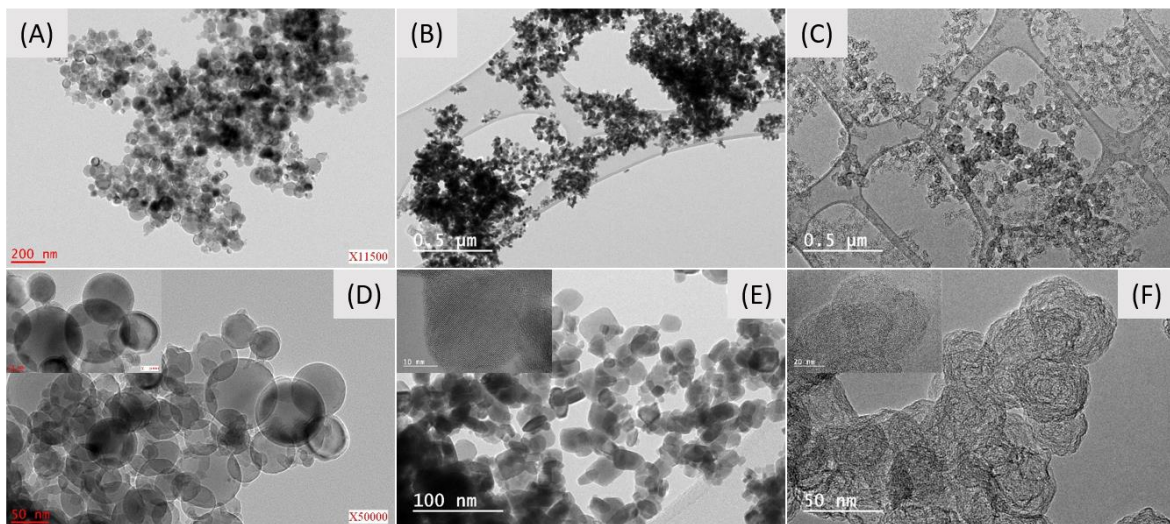


**Figure 3.** Transmission electron microscopy images of (A,D) aluminum, (B,E) tungsten (VI) oxide, and (C,F) highly-conductive carbon nanopowders.

### 3.2. Characterizations and Properties of the Al/WO<sub>3</sub>/C Energetic Formulations

#### 3.2.1. Sensitivity Properties of the Al/WO<sub>3</sub>/C Energetic Formulations

The different materials were then mixed, using the sonication process described above, in various proportions to form Al/WO<sub>3</sub>/C energetic formulations. An equivalence ratio of 1.4 was set between the fuel and oxidizer ingredients and the concentration of the carbon additive was varied from about 2 to 35 vol. %.

Figure 4 shows the electrical conductivity of the different as-prepared Al/WO<sub>3</sub>/C composite materials as a function of the Ketjenblack carbon concentration. The energetic mixtures were pressed at 31–35% of the TMD except for the mixtures containing 18.80 and 34.25 vol. % of carbon, for which values of 28 and 22% were determined due to the high concentration of low-density carbon. The pristine Al/WO<sub>3</sub> has an insulating character (conductivity < 10<sup>-8</sup> S/cm) due to the insulating alumina layer surrounding the aluminum core and the non-conductive WO<sub>3</sub> phase. The conductivity between 0 and 4.08 vol. % of the highly conductive carbon additive increased significantly by five orders of magnitude (< 10<sup>-8</sup> S/cm vs. 8.79 × 10<sup>-3</sup> S/cm). Subsequently, the conductivity values slightly increased again and reached a plateau at 10<sup>-1</sup> S/cm; namely 1.75, 6.27 and 8.95 × 10<sup>-1</sup> S/cm for 9.88, 18.8 and 35.25 vol. % of Ketjenblack EC-600D carbon, respectively. This jump in conductivity can be interpreted by a percolation phenomenon which is due to the connectivity of the additive nanoparticles to each other. Approximately, the percolation threshold can be determined around 2.5 vol. %, i.e., the concentration for which the distribution of the highly conductive carbon is homogeneous within the Al/WO<sub>3</sub> nanothermite until it builds a continuous three-dimensional conductive network. Al/WO<sub>3</sub>/C energetic mixtures were further investigated for their sensitivity to electrostatic discharge. The spark energy during the test ranged from 0.05 mJ to 10 J by varying the voltage and capacitance of the device. Figure 4 shows the energy values, as a function of the concentration of Ketjenblack carbon in the nanothermite, for which there is no ignition of the composition. In other words, these are the values just above the energy required to ignite the energetic materials. As expected, the curve follows the same trend as that of the electrical conductivity profile as a function of the volume percentage of the Ketjenblack additive in the nanothermite; as expected, we can see a prompt increase with the conductive carbon additive until reaching values that reflect a plateau.

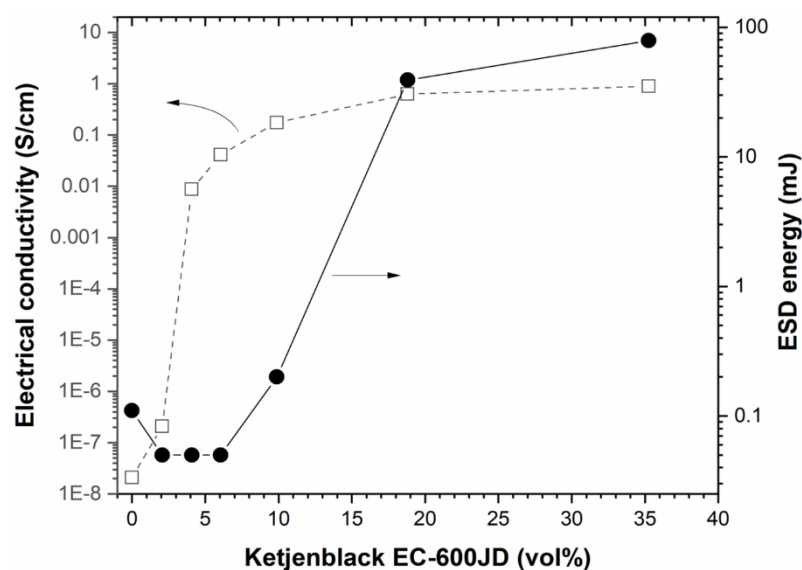


**Figure 4.** Electrical conductivity and electrostatic discharge (ESD) sensitivity threshold of Al/WO<sub>3</sub>/C (C = Ketjenblack) as a function of C concentration (expressed in vol. %).

This result is justified by the fact that adding electrically conductive elements in the nanothermite allows for the rapid evacuation of electrostatic charges and thus avoids the

ignition of the composition by the Joule effect. The more conductive carbon particles there are in the mixture, the easier it is to dissipate the charges, leading to an increase in the ESD value. The conductive carbon nanoparticles tend to create a continuous conductive phase such that the electrostatic current moves through the formulated mixture bypassing the sensitive energetic ingredients. However, a shift of the percolation threshold towards a higher level of carbon nanoparticles rate was observed. Indeed, the percolation threshold was recorded around 12.5 vol. % in this case, which is five times higher than that determined from the curve characterizing the evolution of the electrical conductivity of the energetic formulations (i.e., 2.5 vol. %). This difference can be explained by the following fact: in electrical conductivity measurements, in contrast to ESD tests, the powder is pressed to a density close to 30–40% of the theoretical maximum density (TMD). The shaping of the powder sample under the test conditions promotes connectivity between the particles, which increases the contact area between them. As a result, the charge carriers can self-assemble more easily to create a conductive path and thus facilitate the flow of current (higher electrical conductivity). In ESD sensitivity testing, bulk powders are examined (TMD < 10%) and therefore the contact area between the particles is not as high and the conductivity properties may be lower. This result is not entirely consistent with previous works dedicated to the spark-desensitization of nanothermites by means of conductive component additives [10,12]. When conductive polymers (polyaniline, polypyrrole) are used, the curves are superimposed. The fact that the oxidizer/polymer composites are synthesized, before being mixed with the fuel, probably leads to more intimate and homogeneous fuel/oxidizer/polymer systems, allowing similar percolation thresholds to be obtained between the electrical conductivity and ESD sensitivity curves as a function of the additive concentration.

A scanning electron microscopy (SEM) analysis was performed to determine the conductive carbon-additive dispersion quality within Al/WO<sub>3</sub> nanothermites. Representative SEM pictures of the Al/WO<sub>3</sub>/carbon with a concentration of 3 wt. % (6.05 vol. %) are presented in Figure 5.

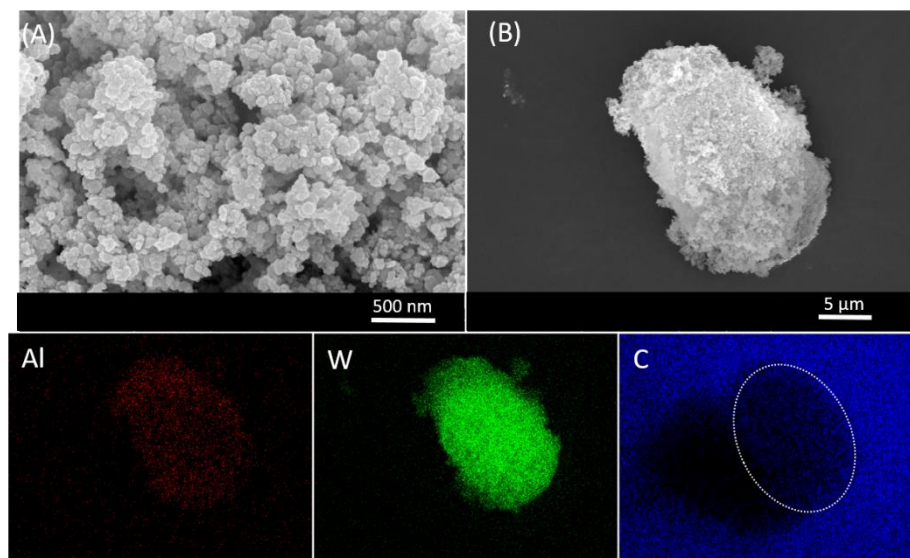


**Figure 5.** Scanning electron microscopy views of the Al/WO<sub>3</sub>/carbon nanothermite (A) at high and (B) low magnification, with a concentration of 3 wt. % (6.05 vol. %) of carbon additive. Equivalence ratio Al/WO<sub>3</sub> was fixed at 1.4. The down line shows the aluminum Al, tungsten W, and carbon C elemental mappings derived from (B) picture.

It can be noted that it is difficult to know which particles represent a given component because the particles have relatively similar sizes and shapes. At best, particles with a quasi-spherical morphology can be attributed to aluminum (Al) in agreement with the



previous TEM analysis. An energy dispersive X-ray spectroscopy (EDX) analysis was performed to verify the chemical composition of the nanothermite (Supplementary Information). Only aluminum (Al), tungsten (W), and carbon (C) were identified. The gold (Au) element observed on the spectrum comes from a layer of Au applied to the surface of the particles to facilitate observation under the electron microscope. To distinguish the particles from each other, elemental mappings of aluminum, tungsten, and carbon were performed (Figure 5). Clearly, Al and W can be observed in the volume of the aggregate studied and seem to be randomly but homogeneously and uniformly distributed. Regarding the carbon element, as the sample was deposited on a carbon-rich adhesive tape, it is observed throughout the picture. However, from a geometric dotted line representation of the location of the aggregate in the image, we can see that the carbon is also present in this specific area and that its distribution is optimal, i.e., over the entire surface of the aggregate. Based on this electron microscope analysis, the homogeneous distribution and intimacy of the Al, WO<sub>3</sub>, and C nanoparticles were evidenced.

To complement the spark ignition sensitivity of nanothermites (the crucial and probably most important criterion in terms of sensitivity), mechanical tests such as friction and impact tests were also carried out on Al/WO<sub>3</sub>/Ketjenblack energetic formulations. The values have been collected in Table 1.

**Table 1.** Impact and friction sensitivity values of Al/WO<sub>3</sub>/Ketjenblack EC-600JD energetic composite materials with respect to the Ketjenblack EC-600JD concentration. A 0 vol. % of carbon additive corresponds to the pristine Al/WO<sub>3</sub> formulation (at an equivalence ratio  $\phi$  of 1.4).

KB EC-600JD (vol. %)	0	2.1	4.1	6	9.9	18.8	34.2
<b>Impact (J)</b>	>100	>100	>100	80	75	90	>100
<b>Friction (N)</b>	<4.9	42	120	144	252	>360	>360

As it can be seen, all Al/WO<sub>3</sub> energetic formulations w/o carbon additive have impacted the sensitivity values at least equal to 75 J. Considering NATO standards, all of them can be considered insensitive since their sensitivity thresholds are well above 40 J [17]. As far as friction sensitivity is concerned, the threshold value increases constantly with the content of Ketjenblack EC-600JD. For example, the value increases from 42 N to over 360 N with 2.06 and 34.25 vol. % additive, respectively. As a reminder, the Al/WO<sub>3</sub> nanothermite, i.e., without carbon, has a threshold value of less than 4.9 N. According to the sensitivity classes established by NATO, Al/WO<sub>3</sub>/C nanothermites can be classified as sensitive, moderately sensitive, and insensitive, with values of 42 N, 80–360 N, and above 360 N, respectively [18].

The phenomenon of desensitization by friction recorded with the introduction of a carbon component in the Al/WO<sub>3</sub> nanothermite can be explained by a physical distancing of the fuel (Al) and oxidizer (WO<sub>3</sub>) components through the carbon nanoparticles. Thus, at a low scale, the intimacy of the mixture, the contact area between Al and WO<sub>3</sub>, and the stoichiometry of the aluminothermy reaction (1) are not maintained, and as a result, the reaction does not occur. Finally, in a global way, Al/WO<sub>3</sub>/Ketjenblack energetic composite materials can be considered as relatively safe to handle or for transport operations.

### 3.2.2. Reactive Behaviours of the Al/WO<sub>3</sub>/C Energetic Formulations

The reactivity properties of Al/WO<sub>3</sub>/Ketjenblack nanothermites were recorded using a high-speed camera after ignition by a flash optical igniter. All video recordings can be seen in the Supplementary Information (videos SI\_a to SI\_f) with the exception of the Al/WO<sub>3</sub> formulation with 34.25 vol. % (20 wt. %) of conductive carbon concentration, for which a low reactivity and an incomplete combustion reaction were observed (not shown here). All the energetic formulations showed an ease of ignition in open environments and were complete because no residues were observed at the end of the burning tests.

However, longer ignition times and lower burning rates were observed for energetic samples with an increasing carbon concentration. As a pyrotechnically inert ingredient, carbon limits the thermite reaction and mitigates its reactive properties [6,19]. The obvious change in the reactive behaviour was observed for a carbon concentration between 9.9 and 18.8 vol. %. While vigorous reactions and dense homogeneous flames characterize energetic systems based on a low amount of carbon (videos SI\_a to e), dispersed incandescent particles were observed for the Al/WO<sub>3</sub> nanothermite formulated with 18.8 vol. % of conductive carbon (video SI\_f). In addition, the reaction time was longer in the latter case than for an amount of carbon ranging from 2 to 9.9 vol. %.

Sequential images of Al/WO<sub>3</sub> nanothermites without and with 18.8 vol. % of carbon additive, extracted from their flame propagation videos, are displayed in Figure 6. The nanothermite consisting of 18.8 vol. % carbon nanoparticles was selected owing to its insensitivities toward mechanical and electrostatic discharge tests, making this handling safe for an operator. In particular, its ESD threshold value was determined to be near 40 mJ, which is two times higher than the energy than a human body can dissipate (8–20 mJ) [2,3,19]. Combustion images confirmed the different reactive behaviours of both energetic systems. While a rapid formation of an intense and luminous fire ball was observed for the Al/WO<sub>3</sub> system (Figure 6A), the Al/WO<sub>3</sub>/Ketjenblack formulation can be described as a projection of uncountable incandescent particles (Figure 6B). Moreover, the reaction time was longer for the latter than for the former since a higher number of images were required to represent the burning event. Obviously, the carbon additive, due to its inert nature, its relatively high content, and its role in suppressing the contact areas between the reactive species (Al and WO<sub>3</sub>), significantly reduces reactive properties.

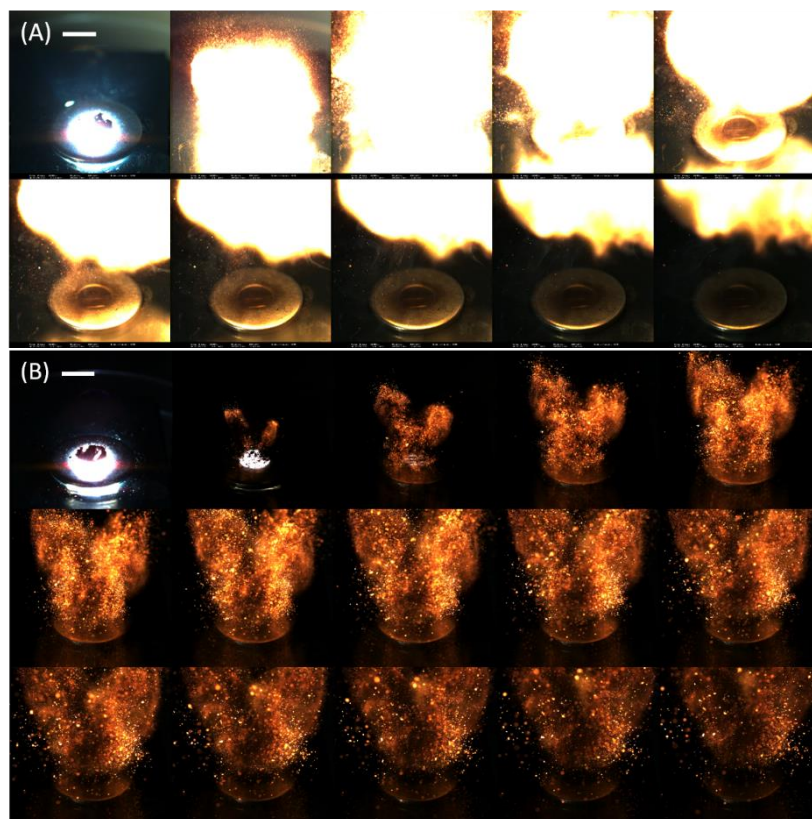


**Figure 6.** Images extracted from the combustion videos of the Al/WO<sub>3</sub>/Ketjenblack energetic material: (A) free of carbon and (B) with 18.8 vol. % of carbon. The equivalence ratio ( $\phi$ ) between Al and WO<sub>3</sub> components was fixed at 1.4. The elapsed time between images was 1 ms and the white scale bar represents 20 mm.

---

The experimental heats of explosion of the Al/WO<sub>3</sub>/Ketjenblack energetic nanocomposites—0 and 18.8 vol. % of carbon—were determined to be equal to 2815 J/g and 1408 J/g, respectively, a loss of 50%, supporting the idea of a less powerful energetic system with carbon. The lost energy may be explained by the consumption of oxygen by the carbon particles and the fact that the corresponding oxidation reaction is less exothermic than the aluminothermal reaction [19].

In summary, compared to previous research mentioning the use of carbon structures to desensitize nanothermites, the Ketjenblack carbon material can also be considered as a promising alternative. This view is based on several facts. First, the concentration of KB EC600JD in Al/WO<sub>3</sub> nanothermites (10 wt. % or 18.8 vol. %) to mitigate the spark sensitivity (ESD sensitivity > 39 mJ) is of the same order of magnitude as the addition of carbon nanotubes (13 vol. %, ESD sensitivity > 100 mJ) [4] and graphene oxide (9.6 wt. %, ESD sensitivity > 24.5 mJ) [6], much lower than carbon fibers (40 wt. %, ESD sensitivity 35 mJ) [8], but slightly higher than nanodiamonds (3 wt. %, ESD sensitivity > 20 mJ) [9]. However, the major advantage of the use of Ketjenblack carbon over the other additives mentioned is the maintenance of an acceptable reactive behavior of the studied system, whereas this one disappears with the addition of carbon fibers and nanodiamonds. For carbon nanotubes and graphene oxide, no reactivity study was conducted by the authors.

#### 4. Conclusions

The present work focused on the spark desensitization of energetic composite materials (nanothermites). For this purpose, a highly conductive additive such as the well-known and versatile Ketjenblack carbon (KB EC-600JD) was introduced into a reference energetic mixture, namely the Al/WO<sub>3</sub> nanothermite. The results showed that an increase in the spark sensitivity threshold and a maintenance of the reactive behaviour (in the open configuration) can be achieved for the energetic system through the addition of 18.80 vol% (10 wt. %) of KB EC-600JD. The spark sensitivity was increased to about 40 mJ—twice the threshold of what can be dissipated by a human body—and the heat of the reaction was maintained at 50% of that of the energetic nanothermite free of carbon component. A desensitization to friction (>360 N vs. <4.9 N) was also recorded with an increasing carbon concentration. These results represent a low-cost and effective route for designing energetic composites with reduced sensitivity.

**Supplementary Materials:** The following supporting information can be downloaded at: [www.mdpi.com/xxx/s1](http://www.mdpi.com/xxx/s1), Video SI: Combustion videos in unconfined configuration of the Al/WO<sub>3</sub>/Ketjenblack energetic nanocomposites with (a) 0, (b) 2.1, (c) 4.1, (d) 6, (e) 9.9, and (f) 18.8% vol. of highly conductive carbon additive, respectively. Equivalence ratio of 1.2.

**Funding:** The author gratefully acknowledges the French National Centre for Scientific Research (CNRS), the French German Research Institute of Saint-Louis (ISL, Saint-Louis, France), and the University of Strasbourg (UNISTRA, Strasbourg, France) for funding.

**Institutional Review Board Statement:**

**Informed Consent Statement:**

**Data Availability Statement:**

**Acknowledgments:** The author expresses his acknowledgements to F. Oudot, Y. Boehrer, B. Lallemand (ISL, Saint-Louis, France), and to L. Vidal (IS2M, Mulhouse, France) for the sensitivity properties determination, the video recordings, and the scanning and transmission electron microscopy analyses, respectively.

**Conflicts of Interest:** The author declares no conflict of interest.

References

References

- 
1. Fischer, S.H.; Grubelich, M.C. Theoretical energy release of thermites, intermetallics, and combustible metals. In Proceedings of the 24th International Pyrotechnics Seminar, Monterey, CA, USA, 27–31 July 1998; pp. 231–286.
  2. Talawar, M.B.; Agrawal, A.P.; Anniyappan, M.; Wani, D.S.; Bansode, M.K.; Gore, G.M. Primary explosives: Electrostatic discharge initiation, additive effect and its relation to thermal and explosive characteristics. *J. Hazard. Mater.* **2006**, *137*, 1074–1078.
  3. Greason, W.D. Electrostatic discharge characteristics for the human body and circuit packs. *J. Electrostat.* **2003**, *59*, 285–300.
  4. Poper, K.H.; Collins, E.S.; Pantoya, M.L.; Daniels, M.A. Controlling the electrostatic discharge ignition sensitivity of composite energetic materials using carbon nanotube additives. *J. Electrostat.* **2014**, *72*, 428–432.
  5. Yan, N.; Qin, L.; Hao, H.; Hui, L.; Zhao, F.; Feng, H. Iron oxide/aluminum/graphene energetic nanocomposites synthesized by atomic layer deposition: Enhanced energy release and reduced electrostatic ignition hazard. *Appl. Surf. Sci.* **2017**, *408*, 51–59.
  6. Bach, A.; Gibot, P.; Vidal, L.; Gadiou, R.; Spitzer, D. Modulation of the Reactivity of a WO<sub>3</sub>/Al Energetic Material with Graphitized Carbon Black as Additive. *J. Energetic Mater.* **2015**, *33*, 260–276.
  7. Kappagantula, K.; Pantoya, M.L. Experimentally measured thermal transport properties of aluminium/ Polytetrafluoroethylene nanocomposites with graphene and carbon nanotube additives. *Int. J. Heat Mass Transf.* **2012**, *55*, 817–824.
  8. Siegert, B.; Comet, M.; Muller, O.; Pourroy, G.; Spitzer, D. Reduced-sensitivity Nanothermites containing manganese oxide filled carbon nanofibers. *J. Phys. Chem. C* **2010**, *114*, 19562–19568.
  9. Pichot, V.; Comet, M.; Miesch, J.; Spitzer, D. Nanodiamonds for tuning the properties of energetic composites. *J. Hazard. Mater.* **2015**, *300*, 194–201.
  10. Gibot, P.; Goetz, V. Polypyrrole material for the electrostatic discharge sensitivity mitigation of Al/SnO<sub>2</sub> energetic composites. *J. Appl. Polym. Sci.* **2021**, *138*, 50752.
  11. Goetz, V.; Gibot, P.; Spitzer, D. Spark sensitivity and light signature mitigation of an Al/SnO<sub>2</sub> nanothermite by the controlled addition of a conductive polymer. *Chem. Eng. Sci.* **2022**, *427*, 131611.
  12. Bohlouli, G.; Wen, Z.; Hu, A.; Persic, J.; Ringuette, S.; Zhou, Y.N. Thermo-chemical characterization of Al nanoparticle and NiO nanowire composite modified by Cu powder. *Thermochim. Acta.* **2013**, *572*, 51–58.
  13. Shen, J.; Qiao, Z.; Zhang, K.; Wang, J.; Li, R.; Xu, H.; Yang, G.; Nie, F. Effects of nano-Ag on the combustion process of Al-CuO metastable intermolecular composite. *Appl. Therm. Eng.* **2014**, *62*, 732–737.
  14. Ferrari, A.C.; Robertson, J. Interpretation of Raman spectra of disordered and amorphous carbon. *Phys. Rev. B* **2000**, *61*, 14095–14107.
  15. Martirosyan, K.S. Nanoenergetic gas-generators: Principles and applications. *J. Mater. Chem.* **2011**, *21*, 9400–9405.
  16. The North Atlantic Treaty Organization. *NATO Standardization Agreement (STANAG) on Explosives, Impact Sensitivity Tests, No.4489*, 1st ed.; NATO: Brussels, Belgium, 17 September 1999.
  17. The North Atlantic Treaty Organization. *NATO Standardization Agreement (STANAG) on Explosive, Friction Sensitivity Tests, No. 4487*, 1st ed.; NATO: Brussels, Belgium, 22 August 2002.
  18. Gibot, P.; Miesch, Q.; Bach, A.; Schnell, F.; Gadiou, R.; Spitzer, D. Mechanical desensitization of an Al/WO<sub>3</sub> nanothermite by means of carbonaceous coatings derived from carbohydrates. *C* **2019**, *5*, 37.
  19. Moureaux, P.; Poyard, J.L. *Phénomènes Électrostatiques — Risques Associés et Prévention*; ED 6354; INRS: Quebec City, Canada, 2019.